RADIATION RESEARCH **114,** 385–398 (1988)

Renal Damage in the Mouse: The Response to Very Small Doses per Fraction

M. C. JOINER AND H. JOHNS

Gray Laboratory of the Cancer Research Campaign, Mount Vernon Hospital, Northwood, Middlesex HA6 2RN, United Kingdom

JOINER, M. C., AND JOHNS, H. Renal Damage in the Mouse: The Response to Very Small Doses per Fraction. *Radiat. Res.* **114,** 385–398 (1988).

Experiments were undertaken to study the effect on the mouse kidney of repeated X-ray doses in the range 0.2 to 1.6 Gy per fraction and neutron doses in the range 0.05 to 0.25 Gy per fraction. A top-up design of experiment was used, so that additional graded doses of d(4)-Be neutrons ($\bar{E}_N$ = 2.3 MeV) were given to bring the subthreshold damage produced by these treatments into the measurable range. This approach avoided the necessity to use a large number of fractions to study low doses per fraction. Renal damage was assessed using three methods: ^{51}Cr-EDTA clearance, urine output, and hematocrit at 16–50 weeks postirradiation. The dose–response curves obtained were resolved best at 29 weeks. However, the results were also examined by fitting second-order polynomials to the data for response versus time postirradiation and using interpolated values from these functions at 29 weeks to construct dose–response curves. This method reduced slightly the variation in the dose–response data, but the interrelationship between the dose–response curves remained the same. The data were used to test the linear–quadratic (LQ) description of the underlying X-ray dose–fractionation relationship. The model fits well down to X-ray doses per fraction of ~1 Gy, but lower X-ray doses were more effective per gray than predicted by LQ, as seen previously in skin [M. C. Joiner *et al., Int. J. Radiat. Biol.* **49,** 565–580 (1986)]. This increased X-ray effectiveness and deviation from LQ are reflected directly in a *decrease* in the RBE of d(4)-Be neutrons relative to X-rays at low doses, since the underlying response to these neutrons is linear in this low-dose region. The RBE decreases from 9.9 to 4.7 as the X-ray dose per fraction is reduced below 0.8 Gy to 0.2 Gy, reflecting an increase in X-ray effectiveness by a factor of 2.1. A model is discussed which attempts to explain this behavior at low doses per fraction.

INTRODUCTION

From the studies of normal tissues and tumors which have been reported so far, it can be concluded that the dose–fractionation response is almost invariably described accurately by the well-known linear–quadratic (LQ) model over the radiation dose range from large single doses down to doses per fraction of about 2 Gy. That this one simple model of radiation response *in vivo* has been found to be widely applicable has improved the interface of radiation biology with clinical radiotherapy, and has given fresh insights into possible ways in which radiation treatment might be improved (*1–8*). The application of LQ relationships *in vivo* has also been supported by biophysical models which suggest a more fundamental basis for an LQ relationship

0033-7587/88 $3.00

applied to cell survival (e.g., (*9, 10*)), although the actual relationship between target cell survival and observed functional deficit *in vivo* is likely to be complex (*11, 12*).

Clearly, the increasingly wide use of the LQ model means that its limitations must be explored, and the current interest in both hyperfraction and accelerated fractionation (e.g., (*13*)) requires that the response of tissues to low doses per fraction (<2 Gy) be examined. There is already an indication that deviations from the LQ model occur at such doses (*14–17*).

Experiments in this dose range are difficult to execute because they require very many fractions to be administered to achieve a measurable end point. For example, Stewart *et al.* (*16*) show that it requires at least 80 dose fractions to study X-ray doses of less than 0.8 Gy per fraction in mouse kidney. Such experiments are usually compromised by the need for a short interval between fractions to avoid excessively long overall times, so that repair may be incomplete, and clearly become impractical if the dose per fraction is reduced much further.

These logistical problems in carrying out such experiments are overcome by using a top-up approach (*18*), in which a reduced number of low-dose fractions are followed by an extra "top-up" dose of neutrons to bring the subthreshold damage into the measurable range. This experimental design also enables the effect of different doses per fraction to be studied while maintaining a constant number of fractions, and hence a constant overall time and constant interfraction interval. These factors are therefore the same in every treatment, and so changes in effect reflect only changes in dose per fraction, as required in a rigorous test of the LQ model.

The experiments described in this paper use this top-up technique to examine X-ray effectiveness in the mouse kidney, using doses of 0.2 to 1.6 Gy per fraction. If the LQ model holds in this dose region, a significant fractionation effect would be predicted for kidney ($\alpha/\beta \approx 3$ Gy), amounting to about a 40% *increase* in the total isoeffective X-ray dose as the dose per fraction was reduced from 1.6 to 0.2 Gy. In addition, we also compared these X-ray data with the results from small neutron fractions using 0.05 to 0.25 Gy per fraction.

MATERIALS AND METHODS

Mice and irradiation schedule. Female CBA/Ht/GyfBSVS mice aged 12–16 weeks (19–25 g weight) were irradiated in air without anesthetic. Six animals were allocated to each dose group which received 30 fractions of either 240 kVp X rays or d(4)-Be neutrons in an overall time of 19 days (3 working weeks), using two fractions per day with an interval of 7 h and 10 fractions per week. Three days after receiving their last radiation fraction, all mice received a single top-up dose of d(4)-Be neutrons, to give a total overall treatment time of 22 days. Mice were irradiated bilaterally using a 20 × 13-mm field which included both kidneys. Each radiation dose was split into two immediately consecutive halves, with the mice rotated 180° in between, to improve dose uniformity.

X rays. The irradiation system has been described previously (*19, 20*). 240 kVp X rays were filtered with 1.0 mm Al and 0.25 mm Cu, to give an HVL = 1.3 mm Cu. Dose rate was 1.7 Gy min^{-1}. Blocks of four dose groups were each given 30 fractions of the same X-ray dose, selected from the range 0.2–1.6 Gy per fraction. Four graded single top-up doses of d(4)-Be neutrons were given subsequently to each block of dose groups to produce a complete dose–response curve for each small X-ray dose studied, according to the method of Joiner and Johns (*21*).

Neutrons. Neutrons were produced from the Gray Laboratory van de Graaff accelerator by bombarding a thick beryllium target with 4 MeV deuterons. This gave neutrons with mean energy = 2.3 MeV, dose mean lineal energy = 65.6 keV/μm, and half-value thickness ~ 3.0 cm ICRU muscle (*22, 23*). Dosimetry

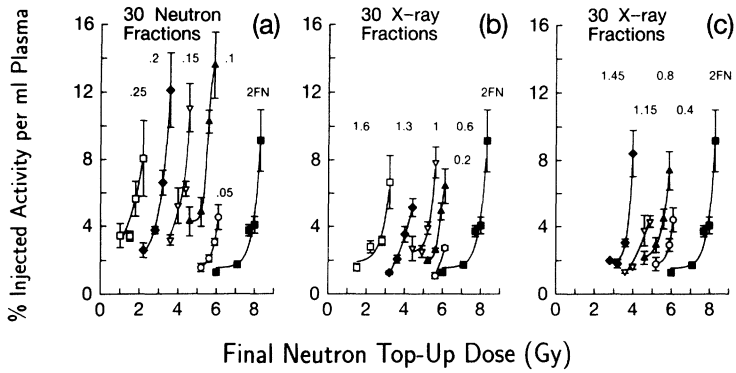

FIG. 1. Residual activity of ^{51}Cr-EDTA measured in plasma samples 1 h after injection, plotted against the final top-up dose of d(4)-Be neutrons. Each dose response curve is for a 30 small fraction "priming" treatment, with dose per fraction shown, followed by a neutron top-up. The dose–response curve to the far right of each panel (marked 2FN) shows a reference response to a large dose of neutrons split into two equal fractions, i.e., zero priming treatment. Errors are standard error of the mean.

was according to the European Protocol (*24*). Doses are quoted as neutron dose alone in agreement with our practice previously (*21, 25*). The γ contamination was 12.2% of the total neutron plus γ dose. Neutron dose rate was 0.5 Gy min^{-1}. Neutrons were given either as two large fractions or as 30 small fractions in the dose range 0.05–0.25 Gy per fraction followed by a large single neutron top-up dose according to the same schedule used with the small X-ray fractions.

Assays. Three assays of renal damage were used: clearance of ^{51}Cr-EDTA, urine output, and hematocrit reduction as described previously (*19, 20, 25, 26*). Mice were assayed every 4 to 5 weeks from 16 to 50 weeks postirradiation.

Isotope clearance. ^{51}Cr-EDTA was used to assess renal clearance by measuring concentration in the blood 1 h after an intraperitoneal injection of 10 μCi ($\approx$200 μg EDTA) given as 0.1 ml of a solution with activity 100 μCi/ml. A single 70 μl blood sample was taken from the orbital sinus and centrifuged for 2 min at 12,000*g*, and plasma samples were then counted for residual γ activity. Results are expressed as the percentage of injected activity per milliliter of plasma at 1 h after injection.

Hematocrit. Progressive reduction in hematocrit is a consequence of renal irradiation (*26*) and is dose dependent. Hematocrit was measured after centrifugation in the blood sample taken during the isotope clearance assay.

Urine output. Urination frequency, expressed in urination events per 24-h period, is a convenient measure of the urine output, which increases with time in a dose-dependent manner after renal irradiation (*19*). Mice were housed in individual wire-bottomed cages for 24-h periods, and urination events were recorded on a paper roll moving at 15 cm h^{-1} below the bottom of the cages.

RESULTS

In agreement with our practice previously, we chose initially to analyze the data at the time when maximum resolution and differentiation of the dose–response curves were obtained for each assay (*20, 21, 25, 27*). This procedure is justified since it has been demonstrated that the time of assay has no significant influence on either the shape of the underlying dose–response relationship (as determined by the α/β ratio) or RBE values measured for neutrons (*20, 21, 25*). Best resolution in these experiments was obtained at 29 weeks postirradiation, and Figs. 1, 2, and 3 show the data obtained with the three assays. Smooth dose–response curves were fitted to the data points with least-squares regression, using a generalized logit function. These curves

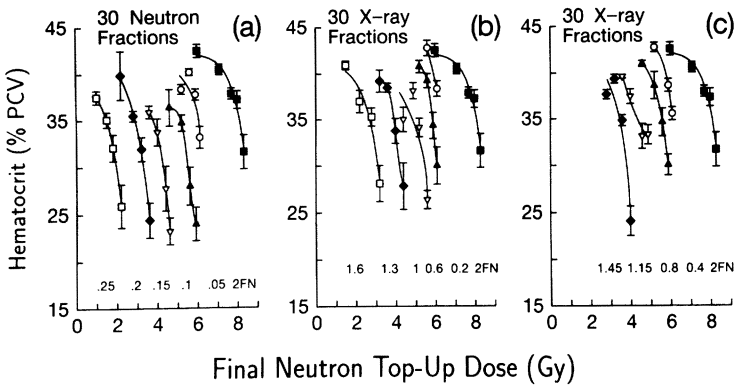

FIG. 2. The hematocrit measured at 29 weeks postirradiation. The explanation of the curves is as for Fig. 1.

appear identical to the lines one would draw through the data "by eye" and have the advantage of being objective fits.

Each dose–response curve in Figs. 1, 2, and 3 is made up of dose groups (mean ± SE of six mice) which received 30 identical initial "priming" treatments of either X rays or neutrons. The dose per fraction given is shown next to each curve. These dose groups then received graded single neutron top-up doses so that full dose–response curves were obtained as a function of neutron top-up dose. These curves are shifted left toward lower top-up doses as the initial dose per fraction gets larger, reflecting an increasing (although subthreshold) effect of dose in each of the 30 small fractions. The curve on the far right of each panel (labeled 2FN) in Figs. 1, 2, and 3 shows the response to a total dose of neutrons *alone* (i.e., *no* initial priming treatment) given in two fractions separated by 1 week. This curve provides a reference for zero priming treatment against which to measure the left-shift of the other curves for priming treatment plus top-up. *Single* neutron doses (as used for the top-ups) were not

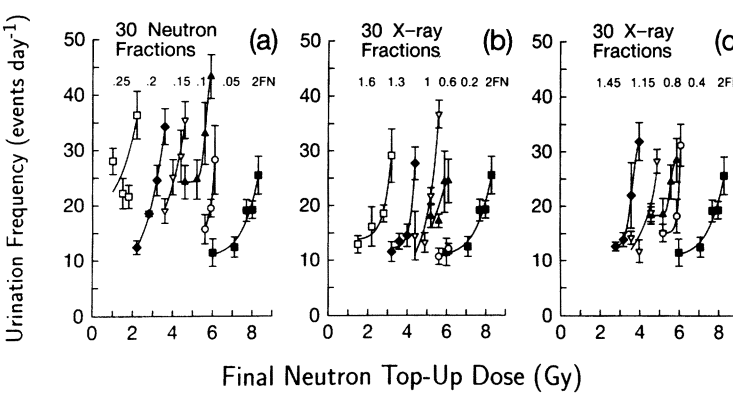

FIG. 3. The urination frequency measured at 29 weeks postirradiation. The explanation of the curves is as for Fig. 1.

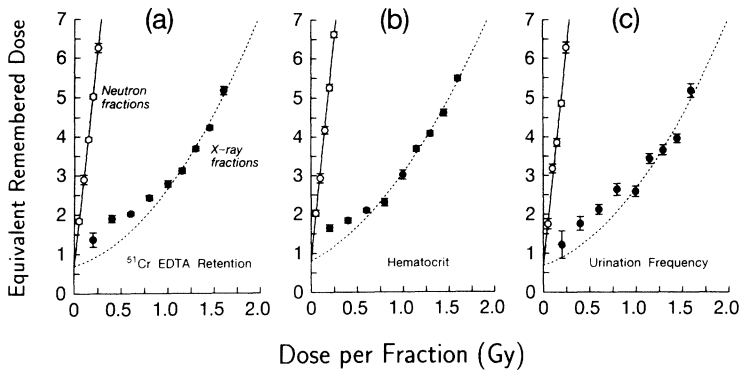

FIG. 4. Equivalent remembered dose (see text) plotted against dose per fraction given in the 30 small neutron (○) or X-ray fractions (●). Each point shows a mean value ± standard error of the mean. Lines are fits to the data points by least-squares regression. Solid line, linear fit to neutron data. Dashed line, linear–quadratic fit to X-ray data in the range 1–1.6 Gy per fraction (see text).

used in the reference curve due to a dose-limiting gut tolerance for large single irradiations (*21*).

Underlying Effect of the Small Dose Fractions

The technique for deriving the underlying effect per fraction in terms of an equivalent remembered dose (ERD) has been explained in detail (*18*). Joiner and Johns (*21*) have also discussed how to implement this method to analyze renal function data in an experimental design identical to that described here.

The ERD is the leftward displacement of each of the dose–response curves in Figs. 1, 2, and 3 relative to the reference curve for two fractions of neutrons alone (2FN) and is a measure of the total effect of the 30 small dose fractions in units of equivalent neutron dose. Since the response of mouse kidney to d(4)-Be neutrons has an α/β ratio of ~20 Gy, which means an almost linear underlying neutron response, the ERD is almost directly proportional to the total underlying effect (or −log[target cell survival]) of the small dose fractions.

For each small dose per fraction in Figs. 1, 2, and 3, the individual ERD was determined for *each mouse* in the dose–response curve by using the fitted 2FN reference curve to determine the equivalent neutron reference dose at the particular response of that animal. The ERD was then calculated by subtracting the neutron top-up dose for that mouse from this reference dose. No dependence of ERD on level of effect was found in this study and so mean ERD and standard error were calculated for all the mice in each dose–response curve.

Figure 4 shows the mean ERD as a function of X-ray or neutron dose per fraction. The pattern of response is very similar for all three assays although the urination frequency assay gave somewhat more variable results, as noted previously (*21*). The data for the small neutron fractions clearly fit a linear relationship with dose, and the straight lines drawn on the diagrams were determined by least-squares linear regres-

TABLE I

Values of the Parameters in the Linear–Quadratic Model

	X rays α/β *(Gy)*	*Neutrons* α/β *(Gy)*	*Notional limiting RBE at low doses* (α_N/α_X)	*Parameters in the "induced repair" model*	
				g	d_c *(Gy)*
ERD vs dose/fraction (Fig. 4)[a]					
EDTA clearance	2.81 ± 0.67 (1.48–4.14)	—[b]	13.2 ± 1.1 (11.1–15.3)	—	—
Hematocrit	1.70 ± 0.36 (0.99–2.42)	—[b]	15.6 ± 1.5 (12.6–18.6)	—	—
Urination frequency	4.9 ± 2.7 (−0.4–10.2)	—[b]	11.3 ± 1.4 (8.6–14.1)	—	—
All available RBE data (Fig. 7)	2.17 ± 0.33 (1.51–2.82)	19.0 ± 6.7 (5.56–32.4)	14.3 ± 1.1 (12.2–16.5)	5.7 ± 4.3 (−2.9–14.2)	0.19 ± 0.07 (0.04–0.34)

Note. Values derived from Figs. 4 and 7. Values ± standard error of the mean; 95% confidence limits are shown in parentheses.

[a] Best fits to *all* the data points.

[b] Analysis not possible since dose range is $\ll \alpha/\beta$ for neutron data.

sion. The intercept on the ERD axis for each assay is similar to that obtained previously (*21*). This displacement from zero occurs because the top-up doses were given as single neutron irradiations, but the reference curve was for a two-fraction neutron treatment. This therefore demonstrates the small but finite dose-sparing as a single 2.3 MeV neutron dose is split into two fractions and shows that even for these high LET neutrons it is possible to detect some repair between two doses. This result indicates that the experimental design would be improved by giving the top-up doses as well as the reference curve as two neutron fractions, since the ERD versus dose curves (e.g., Fig. 4) would then go through the origin. In fact this change has been implemented successfully in more recent studies.

Since ERD is very nearly directly proportional to underlying effect (as defined by −log[target cell survival]), then Fig. 4 may be thought of as a set of inverted "cell survival" curves with the origin at the ERD axis intercept. Thus LQ relationships may be fitted to the X-ray data, of the form

$$(\text{ERD} - I) = W(d(\alpha/\beta) + d^2) \quad (1)$$

where I is the intercept of the line through the neutron fractions with the ERD axis, W is a scaling constant, α/β applies to X rays, and d is the dose per fraction. The X-ray data in Fig. 4 are not well fitted by the LQ relationship. If all points are used in the fit, data points < 1 Gy per fraction tend to lie slightly above the line, thus demonstrating greater X-ray effectiveness, while those >1 Gy per fraction lie slightly below; i.e., the residuals are not randomly distributed with dose. The parameter values for these fits are given for completeness in Table I, although the poor description

of these data by the LQ model should again be emphasized. This is occurring in spite of the very restricted dose range covered (0.2–1.6 Gy per fraction). The lines presented in Fig. 4 show the LQ fit to just the data at 1 Gy per fraction and above. The fit is now good in the range 1–1.6 Gy, but the discrepancy below 1 Gy per fraction is even clearer, again in the direction of increasing X-ray effectiveness.

DISCUSSION

Other Methods of Constructing Dose–Response Curves

In this paper we have described the analysis of the raw data at 29 weeks postirradiation, since for these experiments this was the latest time, giving the most pronounced response, before it became necessary to sacrifice significant numbers of animals entering acute renal failure. Thus the best resolution was obtained, consistent with maximizing the number of animals contributing to the measurements.

Lebesque *et al.* (*28*) showed that for one particular set of data, a "linear" rate of expression of renal damage could be obtained by measuring the slopes of the lines when response, defined as log (% residual EDTA activity), was plotted against time for each dose group. These rate constants could also be used to construct dose–response curves. The analysis of isoeffect doses derived from these curves agreed generally with the analysis performed previously on the same set of data at a given time after irradiation (*20*).

We applied this method to our data but were unhappy with the results. We found that the existence of an additional quadratic component (response $\propto$ time^2) in these response versus time relationships was unpredictable and noticed cases of positive, negative, and zero curvature on the lines. As pointed out by Lebesque *et al.* (*28*), the presence or absence of these higher order terms strongly influenced the value obtained for the linear rate constant. Therefore, since our own set of data was not characterized by a consistent response versus time function, we rejected this approach in favor of using the raw data (Figs. 1, 2, and 3).

A less detailed application of this method was applied subsequently by Stewart *et al.* (*16*) in the analysis of renal response. In their approach, unweighted second-degree polynomials were freely fitted to the values of log (% residual activity) versus time, but rather than using the polynomial coefficients to generate dose–response curves, this procedure was used only as a way of "time averaging" the results, by obtaining interpolated response values read off from the fitted curves at a specific time. The aim of this was to reduce variability in the dose–response curves since fluctuations in function measured at sequential tests would be smoothed out. We have tested this method on the present set of data, and Fig. 5 shows the dose–response curves constructed from interpolated values for the clearance assay, read from the time-smoothed curves at 29 weeks. A comparison of Fig. 5 (smoothed data) with Fig. 1 (raw data) confirms the observation of Stewart *et al.* (*16*) that this procedure does not change the pattern of response. For our own data, the dose–response curves are smoothed slightly, but overall no change in position of the dose–response curves or reduction in the errors on individual dose groups was found. We therefore felt again that it was preferable to use the original dose–response curves (Figs. 1, 2, and 3) for

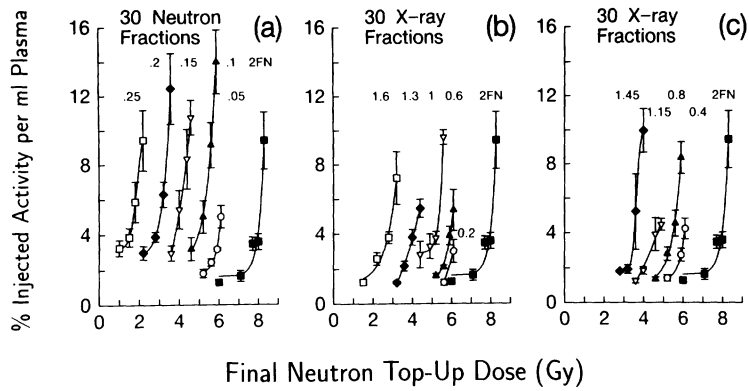

FIG. 5. Data interpolated at 29 weeks, from the second-order polynomial fits to the relationship between log[residual activity/ml plasma] and time (see text). The explanation of the curves is as for Fig. 1. This method of handling the data produces almost identical dose–response curves to those in Fig. 1.

subsequent analysis, which would then remain as closely linked as possible to the original measurements.

We have also looked at the influence of assay time on the ERD measurements in Fig. 4. Analysis at 41 weeks postirradiation demonstrated the same pattern of ERD versus dose, although the variability was greater since there were fewer mice available for analysis at this time. The lack of influence of assay time on the results obtained is a consistent finding in this system provided that the treatment has been given in an overall time of <1 month (*16, 20, 21, 25*). In summarizing this section we would therefore suggest that in this particular experimental design, the efficiency of data collection would be increased and the errors reduced by using more dose groups in the experiment but testing only two or three times within 25–35 weeks postirradiation.

Fit to the LQ Model and Estimate of Flexure Dose for X Rays

Joiner *et al.* (*17*) have shown that a sensitive measure of X-ray effectiveness at low doses per fraction is the relative biological effectiveness (RBE) between X rays and high LET neutrons. The RBE is the ratio of X-ray to neutron dose per fraction needed for the same effect. If the underlying neutron response is linear, as in this case (Fig. 4), then the RBE value (as its reciprocal) reflects exactly the relative effectiveness per gray of that X-ray dose. Relative effectiveness per gray may be defined as the slope of the chord joining the origin of an X-ray cell survival curve to the X-ray dose point on that curve. An advantage in using this approach is that unknown artifacts which might appear in the top-up technique should be similar for both the small X-ray dose fractions and the small neutron dose fractions, and so should be cancelled out in the RBE.

Since equivalent ERD values imply an equivalent effectiveness of the initial treatments (*18*), then RBE values were calculated from Fig. 4 as the ratio of X-ray to neutron dose per fraction required to give the same mean ERD. The RBE values obtained in this way are shown in Fig. 6. Each data point was derived by taking each

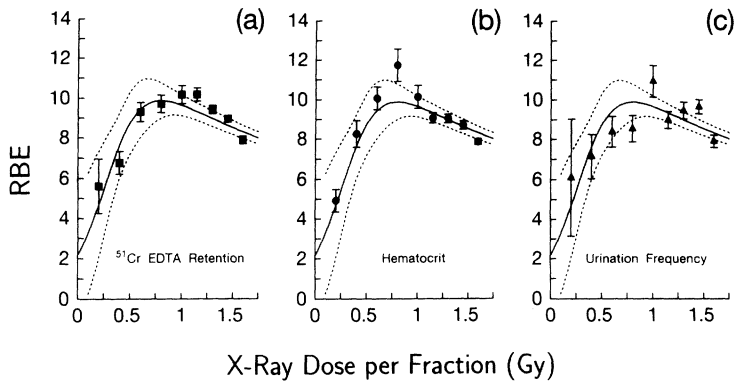

FIG. 6. RBE between X rays and neutrons determined from the data in Fig. 4. Points are means ± standard error. The data indicate decreasing RBE below 0.8 Gy per fraction, reflecting increasing X-ray effectiveness as the dose per fraction is reduced. The lines show the best fit to all available data (see Fig. 7) using a model incorporating increasing X-ray sensitivity at decreasing dose per fraction (see Discussion). The dotted lines are the 95% confidence limits on the mean (expected) values for this fit.

X-ray dose point in Fig. 4, calculating the equivalent neutron dose from the best-fit line through the neutron data, and dividing the X-ray dose per fraction by this value. The standard error on each mean RBE value (Fig. 6) was derived using Fieller's theorem, from the SEM on each mean X-ray ERD value (Fig. 4) and the error on the fit to the neutron data points. All the assays show a reduction in RBE below about 0.8 Gy per fraction, although for urination frequency considered alone, this may not actually be significant.

Since the size of these experiments was necessarily restricted to manageable proportions, we studied here only a restricted X-ray dose range from 0.2 to 1.6 Gy per fraction. However, to measure the flexure dose, i.e., the X-ray dose per fraction below which no significant further increase in total dose would occur with fractionation, or more completely, to assess if and below what dose the LQ model fails, it is necessary to put these data into the context of the renal dose–fractionation relationship over the complete range of doses. Again, this can best be done initially by considering the RBE of X rays relative to high LET neutrons, for three reasons (*21*). First, the RBE versus dose relationship has been found to be independent of the level of effect at which it is calculated, thus allowing different experiments with non-overlapping ranges of effect to be intercompared. Second, all three assays may be included without the need to derive equivalence relationships between the different measures of damage. Third, the top-up data may be compared directly with data from conventional full course fractionation, since RBE is a simple ratio calculation in both cases.

Figure 7a summarizes all the data currently available on the RBE of high LET d(4)-Be neutrons relative to X rays, for renal damage in the mouse. These data are taken from Joiner and Johns (*21*) and Stewart *et al.* (*25*), with the present data added as the closed symbols. There is excellent agreement across the whole dose range, in spite of combining here three separate sets of experiments carried out over 4 years, and three different assays. The reduction in RBE below 0.8 Gy per fraction is seen here clearly as a feature of the whole RBE versus dose relationship and amounts to an increase

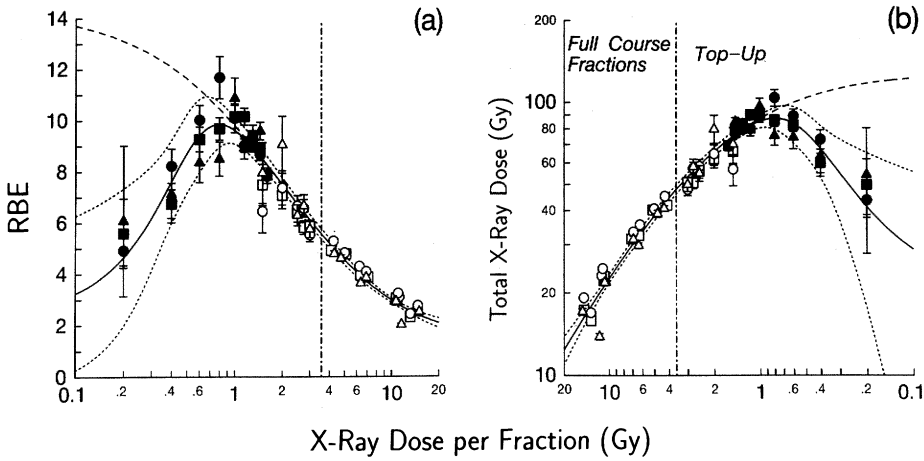

FIG. 7. All available data from comparisons between 240 kVp X rays and d(4)-Be neutrons in the mouse kidney, plotted as (a) RBE between X rays and neutrons or (b) isoeffective X-ray doses to give 3% residual activity, 40% hematocrit, or 15 urination events per day, at 29 weeks postirradiation. Closed symbols, present data. Open symbols, previous data summarized by Joiner and Johns (*21*). Squares, EDTA clearance. Circles, hematocrit. Triangles, urination frequency. The solid lines are the fit to all the data using a model incorporating increasing X-ray sensitivity at very low X-ray doses per fraction, with the dotted lines showing the 95% confidence limits on the mean (expected) values from this fit. Above 1 Gy per fraction, the model rapidly approaches a simple LQ fit, as shown by the dashed line.

in X-ray effectiveness by a factor of 2.1 as the dose per fraction is reduced from 0.8 to 0.2 Gy.

An alternative more common approach to discussing the X-ray dose–fractionation response is presented in Fig. 7b. This shows the total X-ray dose which would be needed in a full course of multiple equal fractions to achieve a given effect, plotted as a function of decreasing dose per fraction. If the LQ model remained valid, this curve would rise with decreasing slope, becoming flat at the lowest doses (dashed line). The effect level chosen was 3% residual activity in the clearance assay at 29 weeks postirradiation, corresponding to a hematocrit of 40% and urination frequency of 15 events/day. For the experiments included in Fig. 7, this response level corresponds to a mean neutron total dose of 7.4 Gy, given in two equal fractions. The data points in Fig. 7b were derived from Fig. 7a at each X-ray dose point, by using the RBE value to obtain an equivalent neutron dose per fraction. By calculating the number of fractions needed of this neutron dose to reach the same underlying effect as 7.4 Gy of neutrons given in two fractions, and assuming that the same number of *X-ray* fractions would be needed at that X-ray dose per fraction, the X-ray total dose was obtained. For top-up experiments, these total X-ray doses calculated in this way are mathematically identical to total X-ray doses extrapolated directly from the neutron top-up doses (see appendix of Joiner and Denekamp (*29*) for this calculation). The closed symbols in Fig. 7b are thus estimated total doses of X rays given in a full course of dose fractions of 0.2–1.6 Gy, which would be equivalent in overall effect to the combination of 30 X-ray fractions of this size followed by a neutron top-up dose as actually given in these experiments. For these calculations, we assumed that the neu-

tron (and hence top-up) response is described by the LQ model, and an α/β of 19 Gy has been used (Table I).

Both approaches in Fig. 7 suggest a deviation of the data from the LQ model below X-ray doses of 1 Gy per fraction, with a flexure dose for mouse kidney in the range 0.8–1.0 Gy per fraction. In the experiments of Stewart *et al.* (*16*), up to 80 dose fractions (without top-up) were used to measure renal damage at doses down to 0.75 Gy per fraction. This study showed a deviation from the LQ model, also in the direction of increased radiation effectiveness, below 2 Gy although some fractionation effect was still seen. These results agreed with previous data of Stewart *et al.* (*20*) using up to 64 fractions (dose per fraction $\sim$ 1 Gy) as reanalyzed by Lebesque *et al.* (*28*). Stewart *et al.* (*16*) have therefore suggested a higher flexure dose of 1–2 Gy per fraction. However, while not excluding a real reduction in repair capacity at decreasing doses per fraction below 2 Gy, they partially explain these results by *incomplete* repair between the lowest dose fractions, since to achieve a constant overall time for all treatment schedules and limited by irradiation within the working day, a 5-h interfraction interval was used for the 80, 64, 60, and 40 fraction treatments (0.75–2 Gy per fraction) compared with $\geqslant$1 day for the lower fraction numbers (2.5–12.5 Gy per fraction). With the top-up technique, we were able to use a minimum interval between fractions of 7 h, even for the lowest doses per fraction, and this more complete repair may explain our lower estimate of flexure dose.

The interfraction interval may be important since Rojas and Joiner (Gray Laboratory Annual Report, 1986) have found a repair half-time ($T_{1/2}$) of 2.1 h for 2-Gy fractions in the mouse kidney, although Stewart *et al.* (*16*) point out that a $T_{1/2} \geqslant 3.3$ h would be needed to explain their data fully using the LQ model.

In the rat spinal cord, Ang *et al.* (*14*) also found that as the dose per fraction was reduced below 2 Gy, the increase in X-ray total dose was much less than predicted from the LQ model as fitted to higher doses per fraction, where the α/β ratio was 1.7 Gy, a low value as in the kidney. Even though these authors used interfraction intervals of only 4 h in some of the treatments with the lowest doses (1.3–1.8 Gy per fraction), as in the kidney, these results could not be adequately explained by incomplete repair using known values of repair half time. Ang *et al.* (*15*) also found a 2 Gy per fraction limit below which no further additional increase in total dose was seen in mouse lip mucosa, although these authors point out that these results contradict those for mouse skin (*17, 30*), where a measurable fractionation effect, in agreement with the LQ model, was seen down to 1 Gy per fraction. However, Joiner *et al.* (*17*) also showed that the LQ model *did* break down in skin below 1 Gy per fraction, with the suggestion that skin tolerance actually *decreased* with decreasing dose per fraction, i.e., that X-ray effectiveness per gray increased as the dose per fraction was reduced from 1 to 0.1 Gy, in direct agreement with the kidney data described in this paper.

In contrast to these data, Parkins and Fowler (*31*) have shown that in the mouse lung, the LQ model describes the X-ray dose–fractionation relationship at least down to 0.6 Gy and possibly right down to 0.15 Gy per fraction, with $\alpha/\beta \sim 3$ Gy. It therefore appears that for several tissues there is a move away from the linear–quadratic prediction toward increasing X-ray effectiveness below 1–2 Gy per fraction, but that this is not a universal phenomenon.

Modeling the Data

To explain the apparent extra sensitivity of mouse skin to X rays at very low doses per fraction, we had speculated previously (*17*) that sensitive phases of the cycle would be continuously replenished with cells by cell cycle progression and redistribution between low-dose fractions. As the dose per fraction was increased above about 0.8 Gy, this replenishment would be gradually prevented by radiation-induced cell-cycle blocking and thus the overall response would then be determined more and more by cells in resistant phases, the sensitive cells having been killed in the first few fractions. However, in kidney, the labeling index is known to be low (~0.3%) as confirmed recently by Wilson *et al.* (*32*) using bromodeoxyuridine incorporation and flow cytometry. There is evidence (G. D. Wilson, personal communication) that this results from normal cell cycle times (~1 day) but with very few cells in cycle. This makes it doubtful that cell kinetics can adequately explain the increase in X-ray sensitivity below 0.8 Gy per fraction.

If incomplete repair between fractions were the explanation, then since we kept the number of fractions *and* the interfraction interval constant for *all* doses per fraction, this would imply that the *repair rate* was decreasing (increasing $T_{1/2}$) rapidly with decreasing dose per fraction. To explain the results it would require effective $T_{1/2}$ values of about 2 h at 1.0 Gy, 3 h at 0.8 Gy, 6 h at 0.6 Gy, 17 h at 0.4 Gy, and 200 h at 0.2 Gy per fraction. If this increase in $T_{1/2}$ was due to repair saturation, this might imply much less availability of repair mechanisms at the lower doses. We therefore postulated that increasing repair capacity might be gradually induced as the dose per fraction is increased from 0 to 0.8 Gy. Induced repair of radiation damage has been reported in human lymphocytes as a result of preexposure to X rays (*33*), but with doses of 0.01 Gy which are very much smaller than used in the present work. Additionally, to date this effect has not been reported in any other mammalian tissues. However, it is worth pursuing such a tenuous argument since it turns out that the simplest model that can be constructed from this reasoning fits these kidney data well, as shown below.

Let cell survival or underlying effect ($-\log_e$SF) be described by the LQ equation

$$-\log_e(\mathrm{SF}) = \alpha d + \beta d^2. \tag{2}$$

Let α decrease with increasing dose per fraction (due to induced repair?) according to the equation

$$\alpha = \alpha_0(1 + g.\exp(-d/d_c)). \tag{3}$$

For zero X-ray dose per fraction ($d = 0$), $\alpha = \alpha_0(1 + g)$ and hence g is a factor of "extra" sensitivity, compared with the high dose response ($d \gg d_c$) where $\alpha = \alpha_0$. d_c is a constant, i.e., a "critical dose for repair stimulation" lying somewhere in the range 0–0.8 Gy. We chose to vary α in this fashion rather than β, since the extreme changes in effect (i.e., $-\log_e$SF) were required at very low doses where the αd term in Eq. (2) dominates over βd^2. However, it is also worth noting at this point that the value of α, i.e., the initial slope on a survival curve, and the value of β in Eq. (2) are both strongly dependent on the proportion of initial lesions allowed to repair (*9, 10*).

Equation (3) was incorporated into the equation relating RBE to X-ray dose per fraction (*21*) and fitted to the data of Fig. 7a using weighted nonlinear least-squares

regression. Alternatively the expected relationship between X-ray total dose and dose per fraction, based on the LQ model (Eq. (2)), may be modified with Eq. (3) and fitted to Fig. 7b to give the same result. The solid lines in Fig. 7 show the good fit to the data with this simple model, with parameter values in Table I. This line is also reproduced in Fig. 6. The unmodified LQ model is shown as a dashed line in Fig. 7; this joins the fit from the "induced repair" model (solid line) above 1.3 Gy per fraction and thus the value of α/β from this model gives the best estimate of this parameter for X-ray doses per fraction > 1.3 Gy. The value of α/β obtained in this way (Table I) was 2.2 Gy (95% CL 1.5–2.8 Gy) and is slightly lower than the value of 3.0 quoted from our analysis of renal RBE data previously (*21*), i.e., just the open symbols in Fig. 7, but agrees well with the value of 2.3 Gy from the latest independent study (*16*).

CONCLUSIONS

The results presented here for renal damage in the mouse support the proposition that the LQ model describes well the dose–fractionation relationship in a wide variety of normal tissues, down to X-ray doses of 2 Gy per fraction. In the range 1–2 Gy per fraction, data from the literature cast some doubt on the applicability of the LQ model. Each tissue should be considered separately, but the data in this paper support the use of the LQ model for the mouse kidney in this dose range, provided that the time between fractions exceeds 7 h. Below 1 Gy per fraction we have shown here that the LQ model fails drastically in kidney, in agreement with our previous findings in skin (*17*), with a substantial increase in X-ray effectiveness as the dose per fraction is reduced below 0.8 Gy.

ACKNOWLEDGMENTS

This work was supported entirely by the Cancer Research Campaign. We are also grateful to Dr. Howard Thames for suggestions regarding the modeling of these data.

RECEIVED: September 18, 1987; REVISED: November 6, 1987

REFERENCES

1. H. R. WITHERS, L. J. PETERS, H. D. THAMES, and G. H. FLETCHER, Hyperfractionation. *Int. J. Radiat. Oncol. Biol. Phys.* **8,** 1807–1809 (1982).
2. H. R. WITHERS, H. D. THAMES, and L. J. PETERS, A new isoeffect curve for change in dose per fraction. *Radiother. Oncol.* **1,** 187–191 (1983).
3. J. F. FOWLER, What next in fractionated radiotherapy? *Br. J. Cancer.* **49,** 285–300 (1984).
4. J. F. FOWLER, Fractionated radiation therapy after Strandqvist. *Acta Radiol.* **23,** 209–216 (1984).
5. H. D. THAMES, An incomplete repair model for survival after fractionated and continuous irradiations. *Int. J. Radiat. Biol.* **47,** 319–339 (1985).
6. R. G. DALE, The application of the linear quadratic dose effect equation to fractionated and protracted radiotherapy. *Br. J. Radiol.* **58,** 515–528 (1985).
7. R. G. DALE, The application of the linear quadratic model to fractionated radiotherapy when there is incomplete normal tissue recovery between fractions, and possible implications for treatments involving multiple fractions per day. *Br. J. Radiol.* **58,** 919–927 (1986).
8. J. F. FOWLER, Short and long fractionated schedules in radiotherapy and a proposed improvement. *Br. J. Radiol.* **60,** 777–779 (1987).
9. S. B. CURTIS, Lethal and potentially lethal lesions induced by radiation: A unified repair model. *Radiat. Res.* **106,** 252–270 (1986).

10. D. T. GOODHEAD, Saturable repair models of radiation action in mammalian cells. *Radiat. Res.* **104,** S58–S67 (1985).
11. T. E. WHELDON, A. S. MICHALOWSKI, and J. KIRK, The effect of irradiation on function in self-renewing normal tissues with differing proliferative organisation. *Br. J. Radiol.* **55,** 759–766 (1982).
12. T. E. WHELDON and A. S. MICHALOWSKI, Alternative models for the proliferative structure of normal tissues and their response to irradiation. *Br. J. Cancer* **53,** 382–385 (1986).
13. M. I. SAUNDERS and S. DISCHE, Radiotherapy employing three fractions in each day over a continuous period of 12 days. *Br. J. Radiol.* **59,** 523–525 (1986).
14. K. K. ANG, A. J. VAN DER KOGEL, and E. VAN DER SCHUEREN, Lack of evidence for increased tolerance of rat spinal cord with decreasing fraction doses below 2 Gy. *Int. J. Radiat. Oncol. Biol. Phys.* **11,** 105–110 (1985).
15. K. K. ANG, W. LANDUYT, F. XU, L. VANUYTSEL, and E. VAN DER SCHUEREN, The effect of small radiation doses per fraction on mouse lip mucosa assessed using the concept of partial tolerance. *Radiother. Oncol.* **8,** 79–86 (1987).
16. F. A. STEWART, Y. OUSSOREN, A. LUTS, A. C. BEGG, L. DEWIT, J. V. LEBESQUE, and H. BARTELINK, Repair of sublethal radiation injury after multiple small doses in mouse kidney: An estimate of flexure dose. *Int. J. Radiat. Oncol. Biol. Phys.* **13,** 765–772 (1987).
17. M. C. JOINER, J. DENEKAMP, and R. L. MAUGHAN, The use of top up experiments to investigate the effect of very small doses per fraction in mouse skin. *Int. J. Radiat. Biol.* **49,** 565–580 (1986).
18. M. C. JOINER, The design and interpretation of top up experiments to investigate the effects of low radiation doses. *Int. J. Radiat. Biol.* **51,** 115–130 (1987).
19. M. V. WILLIAMS and J. DENEKAMP, Sequential functional testing of radiation-induced renal damage in the mouse. *Radiat. Res.* **94,** 305–317 (1983).
20. F. A. STEWART, J. A. SORANSON, E. L. ALPEN, M. V. WILLIAMS, and J. DENEKAMP, Radiation-induced renal damage: The effects of hyperfractionation. *Radiat. Res.* **98,** 407–420 (1984).
21. M. C. JOINER and H. JOHNS, Renal damage in the mouse: The effect of d(4)-Be neutrons. *Radiat. Res.* **109,** 456–468 (1987).
22. R. L. MAUGHAN, A. S. HALL, M. J. ROPER, B. D. MICHAEL, and J. F. FOWLER, The use of a 4 MV Van de Graaff accelerator as a fast neutron source for radiobiology at the Gray Laboratory. In *Radiation Protection: 4th Symposium on Neutron Dosimetry, Neuherberg* (G. Burger and H. G. Ebert, Eds.), EUR 7448, Vol. 2, pp. 5–15. Commission of the European Communities, Luxembourg, 1981.
23. M. FOLKARD, Determination of d(3)-Be and d(4)-Be neutron spectra using a recoil proton spectrometer. *Phys. Med. Biol.* **31,** 135–144 (1986).
24. J. J. BROERSE, B. J. MIHNHEER, and J. R. WILLIAMS, European protocol for neutron dosimetry for external beam therapy. *Br. J. Radiol.* **54,** 882–898 (1981).
25. F. A. STEWART, J. A. SORANSON, R. L. MAUGHAN, E. L. ALPEN, and J. DENEKAMP, The RBE for renal damage after irradiation with 3 MeV neutrons. *Br. J. Radiol.* **57,** 1009–1021 (1984).
26. E. L. ALPEN and F. A. STEWART, Radiation nephritis and anaemia: A functional assay for renal damage after irradiation. *Br. J. Radiol.* **57,** 185–188 (1984).
27. M. V. WILLIAMS and J. DENEKAMP, Radiation induced renal damage in mice: Influence of overall treatment time. *Radiother. Oncol.* **1,** 355–367 (1984).
28. J. V. LEBESQUE, F. A. STEWART, and A. A. M. HART, Analysis of the rate of expression of radiation induced renal damage and the effects of hyperfractionation. *Radiother. Oncol.* **5,** 147–157 (1986).
29. M. C. JOINER and J. DENEKAMP, Evidence for a constant repair capacity over 20 fractions of X-rays. *Int. J. Radiat. Biol.* **49,** 143–150 (1986).
30. B. G. DOUGLAS and J. F. FOWLER, The effect of multiple small doses of X-rays on skin reactions in the mouse foot and a basic interpretation. *Radiat. Res.* **66,** 401–426 (1976).
31. C. S. PARKINS and J. F. FOWLER, The linear quadratic fit for lung function after irradiation with X-rays at smaller doses per fraction than 2 Gy. *Br. J. Cancer.* **53,** Suppl. VII, 320–323 (1986).
32. G. D. WILSON, J. A. SORANSON, and A. A. LEWIS, Cell kinetics of mouse kidney using bromodeoxyuridine incorporation and flow cytometry: Preparation and staining. *Cell Tissue Kinet.* **20,** 125–133 (1987).
33. J. K. WIENCKE, V. AFZAL, G. OLIVIERI, and S. WOLFF, Evidence that the [^{3}H] thymidine-induced adaptive response of human lymphocytes to subsequent doses of X-rays involves the induction of a chromosomal repair mechanism. *Mutagenesis* **1,** 375–380 (1986).